RESEARCH ARTICLE

Characterization of natural organic matter in South African drinking water treatment plants: Towards integrating ceramic membrane filtration

Welldone Moyo[1] [ORCID] | **Machawe M. Motsa[1]** | **Nhamo Chaukura[1,2]** |

Titus A. M. Msagati[1] | **Bhekie B. Mamba[1]** | **Sebastiaan G. J. Heijman[3]** |

Thabo T. I. Nkambule[1]

[1]Institute for Nanotechnology and Water Sustainability, University of South Africa (UNISA), Johannesburg, South Africa

[2]Department of Physical and Earth Sciences, Sol Plaatje University, Kimberley, South Africa

[3]Department of Civil Engineering and GeoSciences, Technical University of Delft, Delft, The Netherlands

Correspondence
Welldone Moyo, Institute for Nanotechnology and Water Sustainability, University of South Africa (UNISA), Johannesburg, South Africa.
Email: moyow@unisa.ac.za

Funding information
University of South Africa (UNISA); Water Research Commission (WRC) of South Africa; National Research Foundation (NRF), South Africa

Abstract

This work presents the first comprehensive investigation of natural organic matter (*NOM*) fraction removal using ceramic membranes in South Africa. The rate of removal of bulk *NOM* (measured as UV_{254} and *DOC* % removal), the biodegradable dissolved organic carbon (*BDOC*) fraction, polarity-based fractions, and fluorescent dissolved organic carbon (*FDOM*) fractions was investigated from water abstracted from drinking water treatment plants (WTPs) in South Africa. Further, mechanisms of ceramic membrane fouling by waters of South Africa were studied. Ceramic membranes removed more than 80% *DOC* from samples from coastal WTPs, whereas for inland plants, the removal was between 60% and 75% of *DOC*. *FDOM* was removed to at least 80% regardless of the site of the plant. The *BDOC* removal by the ceramic membranes was above 85%. The hydrophobic fraction was the most amenable to removal by ceramic membranes regardless of the site of sample abstraction (above 60% for all sites). The freshness index (*β:α*) correlated strongly to UV_{254} removal ($R^2 = 0.96$), thus UV_{254} removal can serve as a proxy for the susceptibility to removal of such class of NOM by ceramic membranes. This investigation demonstrated that ceramic membranes could be a valuable technology if integrated into the existing WTPs.

Practitioner Points

- The removal of bulk parameters by ceramic membrane was greater than unit conventional processes used in all the sampled water treatment plants.
- The hydrophobic polarity-based fraction of NOM was the most amenable to removal by ceramic membranes regardless of the site of the WTP.
- Polarity-based fractions, aromaticity, and initial DOC had a combined influence on the removal of organic matter by ceramic membranes as explained by principal component three.

KEYWORDS

biodegradable dissolved organic carbon, ceramic membranes, fouling mechanism, natural organic matter, spectroscopic indices

INTRODUCTION

South African water treatment plants employ the conventional water treatment processes that include processes such as coagulation/flocculation, disinfection, filtration, and sedimentation. However, these traditional unit processes do not efficiently remove natural organic matter (*NOM*) (around 35% at conventional pH) (Tshindane et al., 2019). Detrimental to water treatment and distribution, *NOM* is the major contributor to the fouling of membranes, is a precursor to the formation of disinfection by-products (DBPs), impacts on the organoleptic properties, accelerates the clogging of the pores of activated carbon, and thus decreases their efficiency, and certain fractions of *NOM* promote biological growth in the distribution networks (Hua et al., 2015; Lobanga et al., 2013; Lyon et al., 2014; Park et al., 2016). Therefore, modifications of the existing water treatment methods or adding new unit processes are required. Such methods could include adsorption, catalysis methods including photocatalysis and photo-Fenton catalysis, and membrane technology.

Membrane technology has great promise for the bulk removal of inorganic and organic pollutants in water. Particularly, nanofiltration (NF) can efficiently remove colloids, particulate matter, and pathogenic bacteria and viruses from water (Metsämuuronen et al., 2014). NF membranes can either be polymeric or ceramic. Although polymeric membranes are generally cheaper than ceramic membranes, they are limited by poor chemical stability, low thermal resistance, diminished mechanical robustness, a short life span, and limited recyclability (Hofs et al., 2011; Pendergast & Hoek, 2011). Ceramic membranes are porous inorganic materials synthesized from oxides of aluminia, titania, zirconia, and of late silicon carbide (Shang, 2014). They are characterized by high selectivity and ability to withstand thermally and chemically aggressive environments (Hofs et al., 2011). However, regardless of more than 20 years of use in the water industry and other separation industries, research on their selectivity in removing specific *NOM* fractions in surface waters is still in its infancy. Moreover, besides limited work from our research group, there is no any other reported information on the use of ceramic membranes for *NOM* removal from South African surface waters.

Therefore, in order to effectively use ceramic membranes in water treatment, it is paramount to understand the character of *NOM* fractions found in source surface waters and removal during membrane filtration. This requires robust and sensitive analytical instrumentation so as to investigate the character and treatability of *NOM* by ceramic membranes in real time.

Current research uses properties such as biodegradable dissolved organic carbon (*BDOC*), fluorescence intensity, molecular weight, polarity, and *UV* absorption to characterize *NOM* (Chen et al., 2017; He et al., 2013; Li et al., 2017; Moyo et al., 2019). The *BDOC* fraction is the fraction of *NOM* that is utilized by bacteria for growth. The polarity of organic matter influences its palatability for uptake by heterotrophic bacteria and is a measure of the degree of chemical change caused by ecological or engineered processes and other metabolic processes (Krzeminski et al., 2019; Liao et al., 2015). Low molecular weight hydrophilic fractions of *NOM* are more palatable to bacteria than high molecular weight hydrophobic fractions (Chen et al., 2014). Fluorescence spectroscopy is a robust tool useful for characterizing *FDOM* in various natural and engineered aquatic systems (Baghoth et al., 2010; Sanchez et al., 2013; Tijani et al., 2014; Zhang et al., 2015). Fluorescence excitation–emission matrix (*FEEM*) spectroscopy has the potential to predict the removal efficiency of *NOM* during drinking water treatment processes (Kastl et al., 2016; Li & Hur, 2017; Wang & Benjamin, 2016). Coupled with multivariate statistical methods such as self-organizing maps (*SOM*), principal component analysis (*PCA*), parallel factor analysis (*PARAFAC*), and fluorescence regional integration (*FRI*), *FEEMs* have been used to identify *NOM* components and provide further insight into the fate of *NOM* in diverse aquatic systems (Bieroza et al., 2011; Henderson et al., 2009; Korak et al., 2013; Sanchez et al., 2013).

Ceramic membranes have been in the water industry for a period spanning more than two decades; however, little is known about their fouling behavior by organic matter from "real waters." The understanding of fundamental fouling mechanisms involved during the filtration process of surface waters is pivotal in order to advance the use of ceramic membranes in water treatment. This work seeks to investigate the effectiveness of ceramic membrane filtration technology in treating surface waters from different water quality regions of South Africa. The objectives were to (1) characterize the *NOM* found in the different region of South Africa using *DOC*, UV_{254}, *FEEM*, *BDOC*, polarity fractions, and fluorescence indices; (2) investigate the removal efficiency of the *BDOC*, *DOC*, *FDOM*, and polarity-based fractions by ceramic membranes through analysis of the differences in the feed and filtrate water quality; (3) evaluate quality indices as predictors of *NOM* removal that can be expected from South African water quality types; and (4) use modeling techniques to investigate the dominant fouling mechanism on ceramic membranes by waters from different water quality sources in South Africa.

METHODS AND MATERIALS

Raw water sources

Five surface water sources, characteristic of the surface water quality types found in South Africa, and serving WTPs were selected (Figure 1): source water supplying the Plettenberg Bay WTP, namely, Keurbooms River in the Southern Cape (PL); Debose Dam, which supplies Veolia WTP and serving Hermanus and parts of Cape Town (H); source water supplying Midvaal WTP, namely, the Vaal river in the North West province (MV); Hezelmere River, which supplies Hezelmere WTP operated by Umngeni water treatment company serving the greater Umngeni municipality (HL); and source water supplying the Mpumalanga province and parts of Polokwane City, namely, Lepelle River (OL). The coastal plants sampled were H, PL, and HL, whereas the inland plants were MV and OL.

Characterization of feed and permeate water

Fluorescence, UV absorbance analysis, and polarity fractionation of NOM

Fluorescence EEMs and absorbance spectra were obtained using a fluorescence spectrometer (Aqualog, HORIBA, Jobin Yvon) to measure the absorbance spectra as well as the determination of EEMs. The applied wavelength range of analysis was 200–800 nm at 2 nm excitation intervals and in the wavelength range 248.58–830.59 nm at 3.28 nm emission intervals. UV absorbance at 254 nm (UV_{254}) measurement of the permeates and concentrate was carried out after every hour during the filtration experiments to determine UV transmission through the membrane. The UV_{254} transmission during the filtration process was calculated as the UV_{254} quotient of permeate to that in the feed water.

The character of the three fractions (hydrophobic, hydrophilic, transphilic) obtained through the polarity rapid assessment method (PRAM) was also analyzed using UV_{254} measurement. The modified polarity rapid assessment method (m-PRAM) was used to partition NOM into three fractions, namely, the hydrophobic (HPO), hydrophilic (HPI), and transphilic (TPI) fractions (Nkambule et al., 2012). A full UV–Vis scan of samples in all filtrate samples was performed for quality assurance and quality control. Readings at representative wavelengths was recorded after each round of cleaning, which included eluting 100 ml of deionized (DI) water.

Parameters such as $SUVA$ were obtained by dividing UV_{254} absorbance by the corresponding DOC value of the sample. Spectroscopic indices such as fluorescence index (FI), freshness index ($\beta: \alpha$), and humification index (HIX) were calculated (Box 1).

BOX 1 **Spectroscopic indices for NOM characterization**

$SUVA \left(\frac{L}{mgM}\right) = \frac{UV_{254}(cm^{-1})}{DOC\left(\frac{mg}{L}\right)} \times 100$

$HIX = \sum I_{435 \to 480} / \left(\sum I_{300 \to 345} + \sum I_{435 \to 480}\right)$

$FI = Em_{470} / Em_{520}$

$\beta: \alpha = Em380 / max(Em420 \to 435)$

$UV_{254} \ Removal \ (\%) = \frac{UV254(feed) - UV254(permeate)}{UV254(feed)} \times 100$

$UV_{254} \ Transmission \ (\%) = \frac{UV254(permeate)}{UV254(feed)} \times 100$
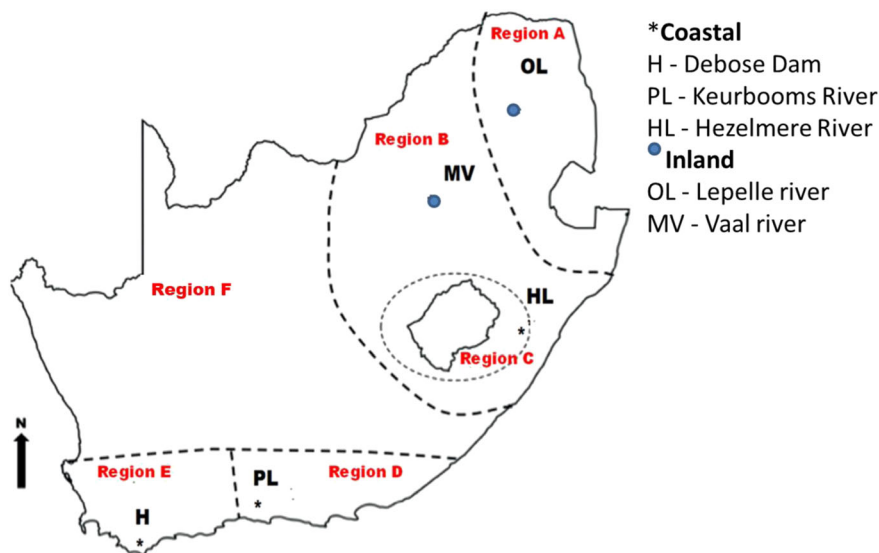

FIGURE 1 The location of selected surface water sources representing different water quality regions of South Africa, adapted from Chaukura et al. (2018). *Coastal plants: H, PL, and HL. Inland plants: MV and OL

PARAFAC modeling of FDOM fraction data

The Aqualog instrument equipped with the SOLO software (Eigenvector Inc.) was used to carry out the *PARAFAC* algorithm analysis following the method by Ndiweni et al. (2019). In short, the EEM dataset is decomposed into a set of trilinear terms and residual array (Equation 1). The goodness of fit of the model and the maximum fluorescence intensities (F_{max}) was obtained through alternating least squares regression procedure.

$$x_{ijk} = \sum_{f=1}^{F} a_{if} b_{jk} c_{kf} + e_{ijk} \qquad (1)$$

where $i = 1 \ldots \ldots I$; $j = 1 \ldots \ldots J$; and $k = 1 \ldots \ldots K$.

The variable x_{ijk} is the *i*th sample fluorescence intensity set at excitation–emission wavelength (*k:j*). The parameter a_{if} contained in the *i*th sample (score) varies with the quantity of the *f*th fluorophore, and the emission–excitation spectrum of the *f*th fluorophore is given by the parameters b_{jk} and c_{kf}, respectively (loadings). The residual variables of model are denoted by the variable e_{ijk}, The sum of components making up the fluorophore is denoted by the variable *F*.

The identification of the fluorescent components emanating from the model was cross-referenced against those reported in literature using the OpenFluor database (Murphy et al., 2014). It should be noted that the results of the identification of components from the model and cross-referenced are indicative not necessarily from the same origin. The split half validation procedure established four components. The F_{max} was used to quantify the validated components from the feed, concentrate, and permeate.

Determination of DOC and BDOC fractionation of NOM

The organic carbon quantity of the BDOC fraction, raw, and permeate of all samples was determined in triplicate using a total organic carbon analyzer (TOC fusion, Teledyne Tekmar). The procedure used by Moyo et al. (2020) was followed in determining the *BDOC*. In brief, biologically active sand (BAS) inoculum was collected from the filter beds of the respective WTP. Sodium thiosulphate solution (0.1 M) was used to wash off excess carbon in the BAS. A steady UV_{254} absorbance was used as an indicator for an effective wash. Thereafter, the BAS was rinsed in DI water, and the supernatant analyzed for fluorescence, UV_{254} and *DOC*, the results of which were used as the baseline. Aliquots of 100 g washed BAS were placed in 500-ml Erlenmeyer flasks, and 300 ml of the

respective raw/permeate water samples was then added. The flasks were then completely covered with aluminum foil and incubated in a water bath set at 22°C for 5 days. Daily measurements of fluorescence, UV_{254}, and *DOC* from each flask were conducted. Control solutions of glucose (5, 8, and 10 mg L^{-1}) dissolved in DI water was subjected to the same experimental conditions.

Membrane and filtration equipment setup

Substrate membranes

Commercial ceramic NF membranes purchased from TAMI, France, were used in these experiments. The membranes had a disc configuration of 90 mm diameter, 2.5 mm thickness, 30% porosity, and an effective filtration area of 0.00563 m^2, and a molecular weight cutoff (MWCO) was 450 Da. The active layer of the received membranes was made of titanium dioxide, TiO_2. The separation layer of the received membranes was made of TiO_2 with a porosity of 30%, as described by the manufacturer, and the other layers are made of alumina (Al_2O_3).

Filtration equipment and operation

The membranes were housed in a circular disc membrane module (TAMI, France), and the system was pressurized by altering the concentrate valve. The feed was circulated by a pump operated at 1100–1180 rrp. Measurements were run under a transmembrane pressure (TMP) of 3 bar and a feed flow of 175 L/h. In the case of DI water, permeates were collected at 10 min intervals and weighed. In the case of the raw water feed, hourly samples were collected from the feed and permeate side for 8 h after equilibration.

Membrane fluxes and water temperature were monitored. The flow rate was correlated to the sample mass, and the flux and temperature-corrected permeability were determined using mass flow equations (Box 2) (Shang et al., 2017):

BOX 2   Mass flow equations

$$v_s = \frac{(M_{sc} - M_c)}{(T_f * 60)/1000}$$

$$\Delta P = \frac{P_f + P_c}{2}$$

$$J = \frac{v_s}{A}$$

$$L_{p, 20oC} = \frac{J}{\Delta P} \cdot \frac{\eta_T}{\eta_{20}} = \frac{J \cdot e^{-0.0239.(T-20)}}{\Delta P}$$

where v_s is the flow rate; M_{sc} and M_c are the mass (g) of the sample container plus permeate sample and the mass (g) of the empty container, respectively; T_f is the temperature of water (°C), ΔP is the measured TMP (bar); P_f (bar) is the feed pressure and P_c (bar) is the concentrate pressure; J is the measured membrane flux ($Lm^{-2}\ h^{-1}$); A is the effective membrane filtration area; $L_{p,20°C}$ is the permeability at 20°C ($Lm^{-2}h^{-1}bar^{-1}$); and η_{20} and η_T are the permeate viscosity at 20°C and at the measured water temperature.

Determination of fouling resistance

The resistance-in-series model gives the best description of membrane fouling behavior (Equation 2):

$$R_t = R_m + R_f = R_m + R_{rev} + R_{irr} = \frac{TMP}{\mu J} \qquad (2)$$

where R_t denotes the summation of all resistance during the membrane process (m^{-1}); the intrinsic membrane resistance is denoted by R_m (m^{-1}); fouling resistance due to fouling resistance is represented by R_f (m^{-1}), including irreversible and reversible resistance (R_{irr} and R_{rev}, respectively); the transmembrane pressure is denoted by TMP, which was held constant at 3 bar in these experiments; the permeate flux is represented by J (m^3/m^2 s); the dynamic viscosity was represented by the variable μ (Pa·s); and J is the permeate flux of the membrane during the filtration process (m^3/m^2 s).

The intrinsic membrane resistance R_m was calculated by determining pure water flux at the onset of the experiment. Thereafter, the total resistance (R_f) of the membranes was determined by filtering for 8 h various feed streams of the surface waters. The permeate mass was recorded at 5-min intervals. The normalized form (R_f/R_m) was used to express the total fouling resistance.

Determination of fouling mechanisms

The fouling mechanisms were determined using the model equations in Box 3. The goodness of fit (R^2) of the plot of time (t) versus $Ln\left(\frac{J}{J_o}\right)$ in the first 2 h was used as a measure of dominancy of complete blocking mechanism. The goodness of fit (R^2) in the first 2 h of the plot of time (t) versus $\left(\frac{J_o}{J}\right)^{\frac{1}{2}} - 1$ was used as a measure of dominancy of standard blocking mechanism. The goodness of fit (R^2) between 2 and 4 h of the plot of time (t) versus $\left(\frac{J_o}{J}\right) - 1$ was used as a measure of dominancy of intermediate blocking mechanism. The goodness of fit (R^2) in the

---

BOX 3 Models to describe fouling mechanisms: (1) complete blocking, (2) standard blocking, (3) intermediate blocking, and (4) cake filtration, respectively (de Angelis et al., 2013)

(1). $J = J_0 e^{-At}$ $\qquad$ $A = K_A u_0$

(2). $J = \frac{J_0}{(1+Bt)^2}$ $\qquad$ $B = K_B u_0$

(3). $J = \frac{J_0}{(1+At)}$

(4). $J = \frac{J_0}{\sqrt{1+Ct}}$ $\qquad$ $C = (2R_r)K_c u_0$

---

last 2 h of the plot of time (t) versus $\left(\frac{J_o}{J}\right)^2 - 1$ was used as a measure of dominancy of cake filtration mechanism.

where the initial and final flux are represented by J_0 and J, respectively; u_o denotes the mean initial filtrate velocity; R_r represents the proportion of resistance of the cake to that of the clean membrane; K_A is the ratio of the membrane surface blocked to the total volume permeated; K_B denotes the reduction in cross-sectional area of the pores due to the particles deposited on the walls per unit of total permeate volume; and K_C is total permeate volume per unit of membrane area.

RESULTS AND DISCUSSION

Removal of bulk parameters by ceramic membranes

The UV_{254} removal by the ceramic membranes was largely constant over time for all WTPs (Figure 2a). This demonstrates the chemical stability and mechanical strength of ceramic membrane operation over time treating water of different physicochemical properties (Table 1). Notably, coastal plants (H and PL) had the highest values for UV_{254} removal (both 80% on average), and UV_{254} removal by inland plants was in the range 55%–60%. The lower UV_{254} removal in inland plants was due to the character of NOM that was probably largely non-UV absorbing and composed mainly of polysaccharides. Interestingly, a similar trend was observed with DOC removal (Figure 2b). Coastal plants (PL and H) removed more than 80% of DOC, whereas inland plants removed between 60% and 75%. Initial UV_{254} values for coastal plants were 0.17, 0.29, and 0.41 cm^{-1} for HL, H, and PL, respectively, whereas inland plants had UV_{254} values of 0.14 and 0.21 cm^{-1} for OL and MV, respectively. Remarkably, the UV_{254} removal efficiency followed the order of magnitude of UV_{254} values at
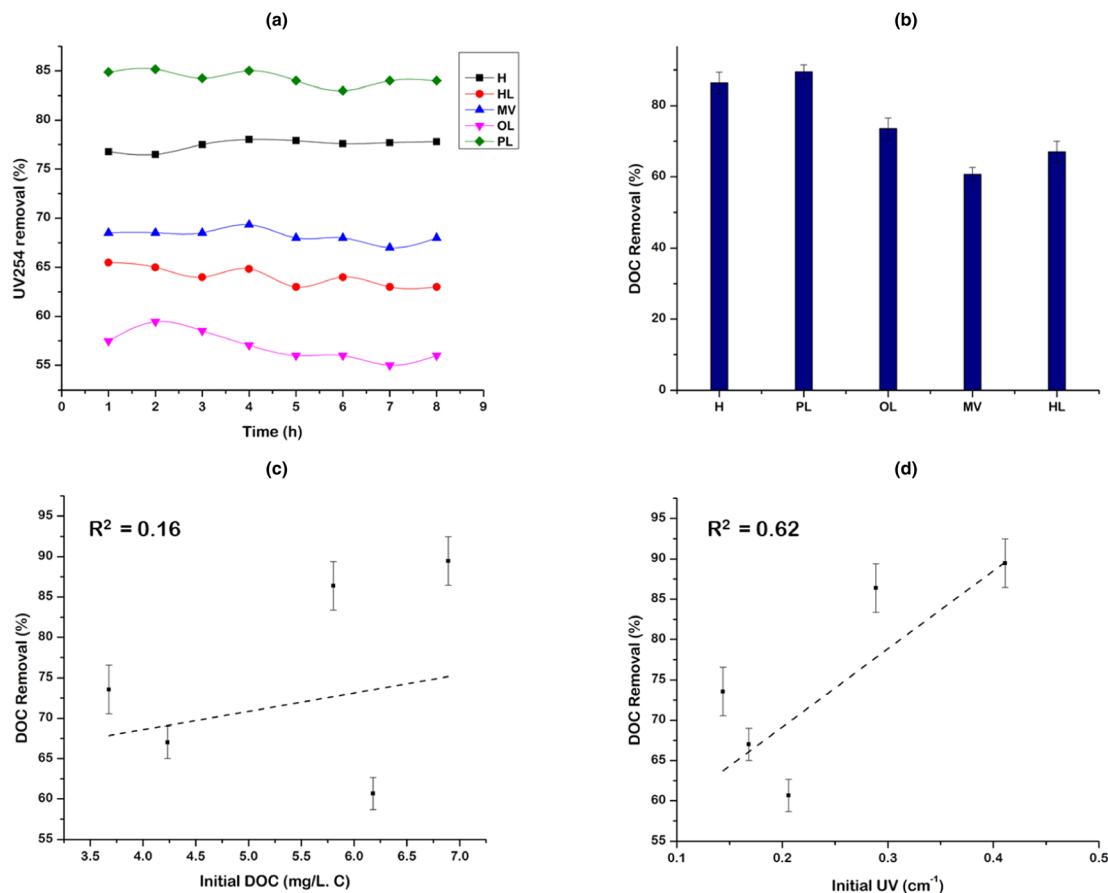
FIGURE 2 Bulk parameter removal by ceramic membranes: (a) UV_{254} removal; (b) DOC removal; (c) correlation between initial DOC and DOC removals and (d) correlation between initial UV_{254} and DOC removal. Experimental conditions: permeate sampling time: every hour; treatment time: 8 h; TMP: 3 bar; Flux: 130 LMH. Sites: H, Debose Dam; PL, Keubooms River; HL, Hezelmere River; MV, Vaal River; OL, Lepelle River

respective sources. UV_{254} is a measure of aromaticity of NOM; therefore, the results suggest that ceramic membranes are selective depending on the aromaticity of NOM. This finding serves as a prediction tool by water treatment companies to forecast the removal efficiency of NOM by determining the UV_{254} values of the source waters.

Figure 2c shows the observed relationship between the initial DOC values of the feed waters and the rate of DOC removal by the ceramic membranes. A poor correlation was observed ($R^2 = 0.16$) between the initial DOC and rate of DOC removal, suggesting the rate of removal of bulk DOC is not entirely dependent on the quantity of DOC in the water sample. Other factors influencing the removal of DOC could be at play, such as the physicochemical characteristics of the NOM in the sample; the physicochemical characteristic of the membrane separation layer; the hydrodynamic properties, including flow rate, TMP; and feed water chemistry, including pH and ionic strength (Metsämuuronen et al., 2014). Therefore, it is not enough to assume greater or lesser removal based

on the initial DOC values alone; there is need for in-depth study of the chemistry of NOM in the feed waters to predict removal by ceramic membranes. This is the premise of this study.

Figure 2d shows the observed relationship between the initial UV_{254} and the rate of DOC rejections by the ceramic membranes. A modest correlation was observed ($R^2 = 0.62$) between the initial UV_{254} and rate of DOC rejections, suggesting that the rejection mechanisms for DOC and UV_{254} correlate to a moderate extent. UV_{254} reflects aromatic and chromophoric NOM, whereas DOC reflects all carbon in a water sampling (including chromophoric and non-chromophoric NOM). Therefore, the modest correlation could be attributed to the NOM characteristics and selective pressures applied on ceramic membranes for NOM treatment.

The $SUVA$ values for the coastal plants were 5.97, 4.97, and 3.97 for PL, H, and HL, respectively, whereas for the inland plants, they were in the range 2–4 (Figure 3). Strong correlations existed between initial $SUVA$ and the rate of DOC removal by the ceramic

TABLE 1 Summary of initial/raw water quality information for the sites with relevant measured parameters

|	**H**	**PL**	**HL**	**MV**	**OL**
pH	5.39 ± 0.3	6.14 ± 0.4	6.51 ± 0.1	7.47 ± 0.3	7.48 ± 0.2
Conductivity (μS/m)	315 ± 14	176 ± 13	179 ± 11	448 ± 10	624 ± 13
UV_{254} (cm^{-1})	0.287 ± 0.03	0.411 ± 0.02	0.168 ± 0.01	0.206 ± 0.01	0.144 ± 0.02
DOC (mg/L.C.)	5.803 ± 0.08	6.892 ± 0.02	4.232 ± 0.07	6.180 ± 0.06	3.676 ± 0.04
BDOC (mg/L.C.)	1.451 ± 0.05	0.882 ± 0.02	1.058 ± 0.01	1.300 ± 0.04	0.772 ± 0.03
F_{max} (a.u.)					
C_1	0.008 ± 0.0002	0.007 ± 0.0003	0.006 ± 0.0001	0.005 ± 0.0002	0.006 ± 0.0002
C_2	0.006 ± 0.0001	0.005 ± 0.0004	0.005 ± 0.0003	0.004 ± 0.0002	0.005 ± 0.0003
C_3	0.005 ± 0.0003	0.003 ± 0.0004	0.003 ± 0.0002	0.003 ± 0.0002	0.004 ± 0.0002
C_4	0.002 ± 0.0002	0.002 ± 0.0001	0.001 ± 0.0002	0.001 ± 0.0001	0.002 ± 0.0001
Polarity-based fractions (cm^{-1})					
HPO	0.082 ± 0.003	0.126 ± 0.002	0.044 ± 0.001	0.068 ± 0.005	0.045 ± 0.004
HPI	0.056 ± 0.002	0.084 ± 0.003	0.029 ± 0.001	0.045 ± 0.002	0.031 ± 0.001
TPI	0.042 ± 0.001	0.063 ± 0.003	0.022 ± 0.001	0.035 ± 0.002	0.024 ± 0.001
Spectroscopic indices					
SUVA	4.974 ± 0.003	5.966 ± 0.002	3.977 ± 0.001	3.331 ± 0.003	3.910 ± 0.001
HIX	0.942 ± 0.03	0.921 ± 0.06	0.890 ± 0.05	0.870 ± 0.03	0.811 ± 0.01
FI	$1.366\pm \pm 0.06$	1.360 ± 0.01	1.604 ± 0.04	1.530 ± 0.06	1.746 ± 0.03
β:α	0.455 ± 0.05	0.429 ± 0.03	0.694 ± 0.04	0.628 ± 0.08	0.822 ± 0.03
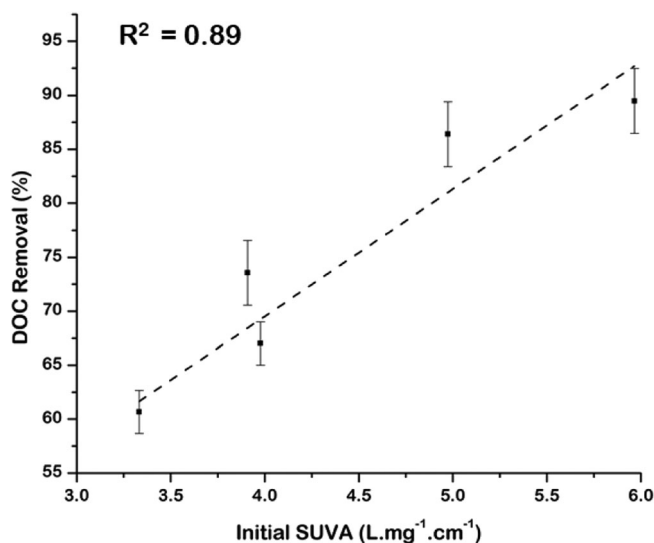
FIGURE 3 Correlation of the initial *SUVA* with *DOC* removal. Experimental conditions: treatment time: 8 h; TMP: 3 bar; flux: 130 LMH. Pooled data from sites: H, Debose Dam; PL, Keubooms River; HL, Hezelmere River; MV, Vaal River; OL, Lepelle River

membranes ($R^2 = 0.89$) (Figure 3). These results were expected because *SUVA* is a quotient of UV_{254} absorbance and *DOC* of the sample. Research has shown that *SUVA* > 4 indicates high hydrophobicity and *SUVA* < 2

is an indication of the predominance of non-humics, low molecular mass compounds and hydrophilicity. *SUVA* between 2 and 4 is exhibited by water that contains roughly an equal mixture of hydrophobic and hydrophilic moieties (Nkambule et al., 2012). Therefore, the results suggest ceramic membranes are particularly selective to hydrophobic *NOM* as demonstrated by high *DOC* and UV_{254} removals by coastal plants. However, extant research has demonstrated that rejection by NF membranes is a physical rejection process determined mainly by the pore size (Chae et al., 2015; Fang et al., 2018). Therefore, the high *DOC* and UV_{254} removals in the coastal plants can only point to larger molecular sizes of the *NOM* in those regions, not necessarily implying higher hydrophobicity, namely, greater rejection by the ceramic NF membranes. Therefore, the selectivity to hydrophobic *NOM* removal by the ceramic membranes deserves further investigation. In general, the hydrophilic fraction of NOM is reported to be recalcitrant to removal by membrane technology compared with the hydrophobic fraction (Metsämuuronen et al., 2014).

Our previous research efforts were directed toward investigating the removal efficiencies of *DOC* using conventional methods (coagulation, sedimentation, filtration, and disinfection) at South African plants including those being investigated in the current research study,

and *DOC* removal efficiencies were in the range −35%–48% (Tshindane et al., 2019). The current study has demonstrated *DOC* removal efficiency of between 60% and 80%; therefore, integrating ceramic membrane technology with the conventional methods should result in greater *DOC* removal.

Removal of fluorescent fractions by ceramic membranes

Components representing universal variance were achieved by pooling *EEM* data from all sources and inputting into the *PARAFAC* model. Therefore, the
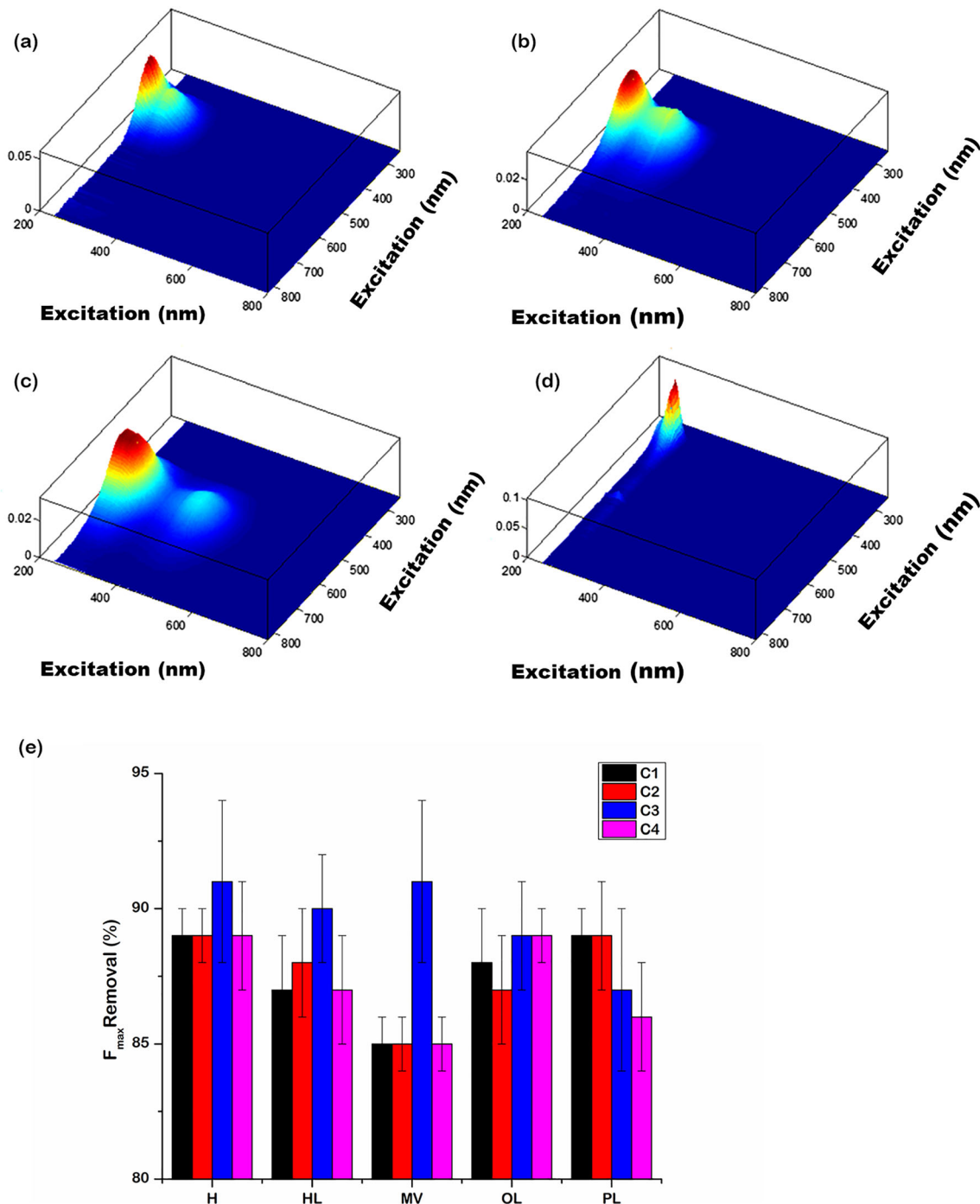

FIGURE 4 Output of the validated components from the *PARAFAC* model (a) (*C1*), (b) (*C2*), (c) (*C3*), and (d) (*C4*), and (e) the F_{max} removal efficiency by ceramic membranes. Experimental conditions: treatment time: 8 h; TMP: 3 bar; flux: 130 LMH. Sites: H, Debose Dam; PL, Keubooms River; HL, Hezelmere River; MV, Vaal River; OL, Lepelle River

produced model culminated from diverse data points. The graphical representation of components is shown in Figure 4a–d. The identification of components was determined by comparing with those in the OpenFluor database that give similarity scores greater than 0.97 (Table 2). All fractions were removed to at least 80% of *FDOM* regardless of the location of the plant. This suggests ceramic membranes have high selectivity toward the removal of fluorescent *NOM* fractions. Raw water from coastal plants had a yellowish-brown coloration, characteristic of the presence of humic and fulvic acid matter. This finding was further corroborated by high F_{max} for components *C2* and *C3*. Notwithstanding, the removal efficiency of these components was strikingly in the same range as the other plants, suggesting pollutant loading had no bearing on the efficiency of their removal by ceramic membranes. Further studies should investigate the dependence of produced water quality and pollutant loads in terms of character and quantity.

Removal of BDOC fractions

The removal of *BDOC* by the ceramic membranes was above 85% with coastal plants—PL (96%) and H (97%) having the highest removal rate (Figure 5a). Similar rates of *BDOC* removal (>90%) by NF membranes have been reported (Escobar & Randall, 2001). Fraction of *BDOC*

TABLE 2 Identification of the derived components from the PARAFAC model

| Component	Similarity score	Component identity	Reference
C1	0.97	Reprocessed organic matter, terrestrial humic like	Wünsch et al. (2017)
max Ex/Em 316/240(292)	0.98	Photo degradation by-products mimicking humic-like matter	Osburn et al. (2012)
C2	0.98	Soil-derived fulvic acid-like	Osburn et al. (2016)
max Ex/Em 336/240(348)			
C3	0.97	Humic acid-like	Cawley et al. (2012)
max Ex/Em 364/240(450)	0.98	Conjugated macromolecular substances of terrestrial origin exhibiting aromatic humic acid-like character	Osburn et al. (2012)
C4	0.99	Tryptophan-like, protein	Murphy et al. (2011)
max Ex/Em 270/270	0.98	Tryptophan-like	Yamashita et al. (2011)
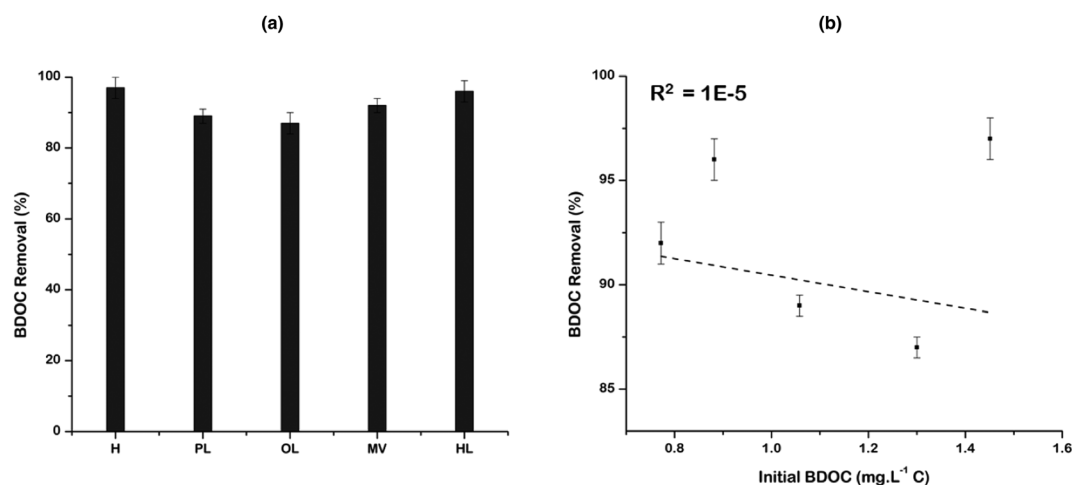
FIGURE 5 Dynamics of BDOC removal (a) *BDOC* removal by ceramic membrane at respective sites; (b) correlation of *BDOC* removal with initial BDOC. BDOC removal (%): 97, 89, 87, 92, and 96 for H, HL, MV, OL, and PL, respectively. Experimental conditions: treatment time: 8 h; TMP: 3 bar; flux: 130 LMH. Sites: H, Debose Dam; PL, Keubooms River; HL, Hezelmere River; MV, Vaal River; OL, Lepelle River

making up the initial *DOC* was in the range 20%–25% (Table 1). The relationship between the *BDOC* in the respective sample correlated well with the initial *DOC* in the same sample ($R^2 = 0.85$). The good correlation was because of the similar technique of analysis and treatment using the total organic carbon analyzer. Interestingly, the trend in the removal efficiencies of *BDOC* removal by ceramic membranes correlated poorly to the initial *BDOC* in the feed water ($R^2 = 1E-5$) (Figure 5b). Similarly, a poor correlation was observed between rate of *DOC* and initial *DOC* in the water sample (Section 3.1). Besides the fact both parameters use similar technique of analysis, the results suggest the rate of removal of *DOC* making of the *BDOC* fraction is not entirely dependent on the quantity of *BDOC* in the water sample. Other factors influencing the removal of *DOC* are at play, such as the physicochemical characteristics of the *BDOC* fraction in the sample; the physicochemical characteristic of the membrane separation layer; the hydrodynamic properties, including flow rate, TMP; and feed water chemistry, including pH and ionic strength (Metsämuuronen et al., 2014). However, the good correlation between the rate of *BDOC* and initial *DOC* implies that the removal of *DOC* can be a predictor of *BDOC* removal by ceramic membranes for the sampled water. The management of the *BDOC* fraction is important because it potentially causes bacterial regrowth in the water distribution system (Terry & Summers, 2018). The *BDOC* fraction is also responsible for the alteration of the physicochemical properties of treated water, affecting the taste and odor, elevating turbidity, causing loss of residual chlorine, and subsequently increasing the formation of DBPs (Li et al., 2017; Vital et al., 2010).

However, it should be noted that the use of membrane-based filtration methods does not completely obliterate posttreatment microbial proliferation. This is because of the passage of the assimilable organic carbon fraction (AOC) through the pores of the membrane even in the NF range (1–10 nm). The AOC represents the low molecular DOC fraction assimilated by specific strains of bacteria for growth, whereas BDOC is a measure of the gross amount of DOC that is biodegraded over a fixed time frame by a microflora of bacteria suspended or fixed on media such as glass beads (Marais et al., 2017). It is vital to measure BDOC because it gives an indication of the potential of bacterial proliferation in the distribution. Ceramic membranes in the NF range are capable of physically removing bacterial cells; however, nutrients beneficial for the bacterial growth and proliferation can easily pass through NF membranes and promote recolonisation in the distribution system (Nescerecka et al., 2018).

Removal of NOM polarity-based fractions

The *HPO* fraction was the most amenable to removal, whereas the hydrophilic fraction was the least removed 30%–47% by ceramic membranes regardless of the location of the WTP (above 60% for all sites) (Figure 6a). The *HPI* fraction is characterized by a low molecular weight and low C/O ratio, indicative of less aromatic carbon content (Lavonen, 2015). The *HPO* fraction is removed from at least 60% by ceramic membranes regardless of the location of the WTP. The high removal of the *HPO* fraction is usually enhanced when the membrane is charged due to charge repulsion between the membrane and the carboxylic and phenolic groups whose pK$_a$ values are in the range 2.5 and 5, whereas the phenolic hydrogens have pK$_a$ values around 9 and 10 (Virtanen et al., 2018). As a result, *HPO* fractions are negatively charged due to
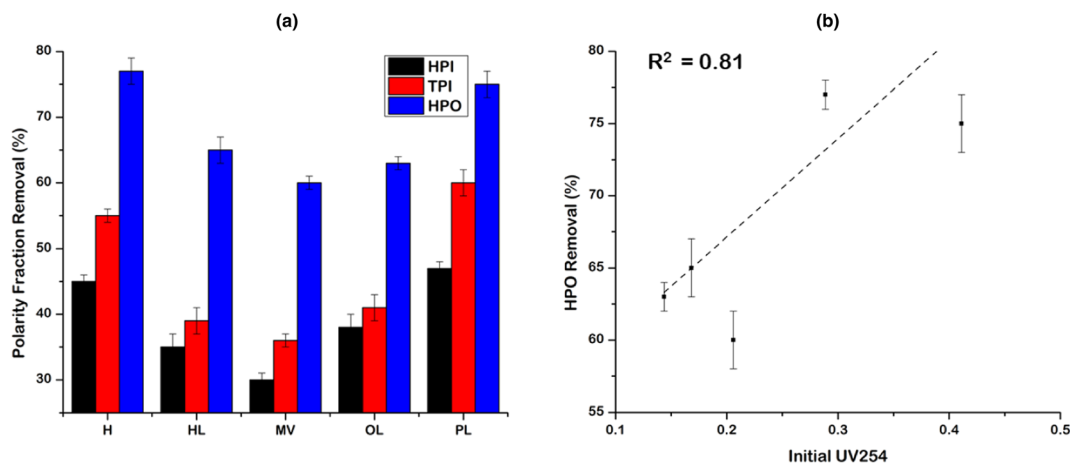

FIGURE 6 NOM polarity fraction removal by ceramic membranes; (b) correlation between *HPO* removal with *UV$_{254}$* removal by ceramic membranes. Experimental conditions: permeate sampling time: every hour; treatment time: 8 h; TMP: 3 bar; flux: 130 LMH. Sites: H, Debose Dam; PL, Keubooms River; HL, Hezelmere River; MV, Vaal River; OL, Lepelle River

ionization of carboxylic groups in the pH range of natural waters (Metsämuuronen et al., 2014). Further, *HPO* fractions have a quasi-linear molecular configuration due to intra-charge repulsion caused by the ionized carboxylic groups (Metsämuuronen et al., 2014; Zularisam et al., 2007). Besides charge repulsion, steric repulsion can play a role in the high rejection of *HPO* compared with *HPI* fraction (Trubetskaya et al., 2016).

The removal efficiency for the *HPO* fraction had a modest correlation with the initial UV_{254} ($R^2 = 0.81$) (Figure 6b). Because UV_{254} is a measure of aromaticity and the *HPO* fraction is composed of aromatic groups with conjugated structures, it was expected that a linear relationship should exist between the initial UV_{254} and *HPO* removal.

The distribution of polarity fractions of the raw water ranged 20%–24%, 28%–31%, and 42%–45% for TPI, HPI and HPO, respectively (Table 1). These results corroborate previously reported studies, which reported NOM in surface water consists of about 50% HPO, the HPI fraction contributing between 25% and 40% and the *TPI* fraction occupying the remainder (Knowles, 2011). Interestingly, polarity-based fraction removal correlated modestly with the initial *DOC* ($R^2 = 0.78$, 0.77, and 0.77 for *HPO*, *HPI*, and *TPI*, respectively) (Figure 7). Therefore, to some extent, initial *DOC* can be a measure of the removal of polarity-based fractions by ceramic membranes.
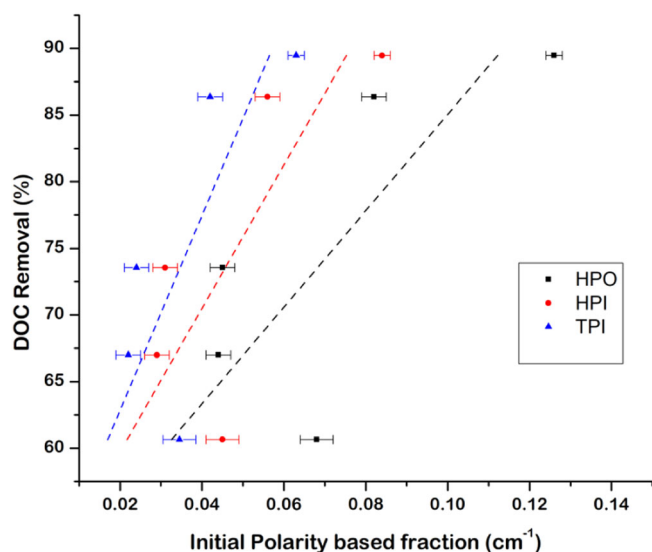

FIGURE 7 Correlation of polarity based fractions and DOC removal by ceramic membranes. Experimental conditions: permeate sampling time: every hour; treatment time: 8 h; TMP: 3 bar; flux: 130 LMH. Pooled data from sites: H, Debose Dam; PL, Keubooms River; HL, Hezelmere River; MV, Vaal River; OL, Lepelle River

Correlation of fluorescent indices at source to removal of bulk parameters by ceramic membranes

UV_{254} removal by ceramic membranes and *HIX* of the feed showed a good correlation ($R^2 = 0.75$) (Figure 8a). The humification index is reported to be good predictor of *NOM* removal efficiency (He et al., 2013; Lidén et al., 2017). Surface waters with high humic substance content are characterized by high *HIX* value (Shang, 2014). Therefore, high *HIX* content water is equally susceptible to removal as waters containing high humic substances can be easily removed by membranes (Shang, 2014). This investigation confirms the aforementioned assertion, whereby higher *HIX* values corresponded to high *UV* removal (Figure 8a). A strong correlation between *FI* and UV_{254} was established ($R^2 = 0.93$) (Figure 8b). Terrestrially derived NOM (*FI* ≈ 1.7) susceptibility to removal by ceramic membranes is less than that of microbial derived NOM (*FI* ≈ 1.4) (Figure 8b). A previous study reported similar findings that when the *FI* index of raw water was greater than 1.5, the NOM in that water was less susceptible to removal by ultrafiltration membranes (Lidén et al., 2017). A strong correlation was observed between the freshness index (*β:α*) and UV_{254} removal ($R^2 = 0.96$) (Figure 8c). Surface water containing aged and condensed humic substances is characterized by low *β:α*; such water is amenable to removal by coagulation or membrane filtration (Lidén et al., 2017). The high correlation of *FI* and *β:α* with UV_{254} removal can be traced to the character of *NOM* with microbial derived *NOM* having the greatest influence to the extent of removal by ceramic membranes. However, very poor correlations existed between the spectroscopic indices and *DOC* removal by ceramic membranes ($R^2 = 0.33$, 0.41, and 0.47 for *HIX*, *FI*, and *β:α*, respectively) (Figure 8d,e). The poor correlation affirms the fact that the indices describe portions of the *DOC* (hence the heterogeneity) not necessarily representative of all the organic matter in the sample.

Figure 9 shows a poor correlation of polarity based fraction removal and *HIX* of the feed water ($R^2 = 0.42$, 0.42, and 0.41 for *HPO*, *HPI*, and *TPI*, respectively). However, modest correlations existed between polarity fractions and *FI* of the feed water ($R^2 = 0.72$, 0.72, and 0.71 for *HPO*, *HPI*, and *TPI*, respectively) again with *β:α* of the feed water ($R^2 = 0.77$; 0.77 and 0.76 for *HPO*, *HPI*, and *TPI*, respectively). Therefore, FI and *β:α* of the feed can be a good predictor of the extent of polarity-based fraction removal by ceramic membranes.
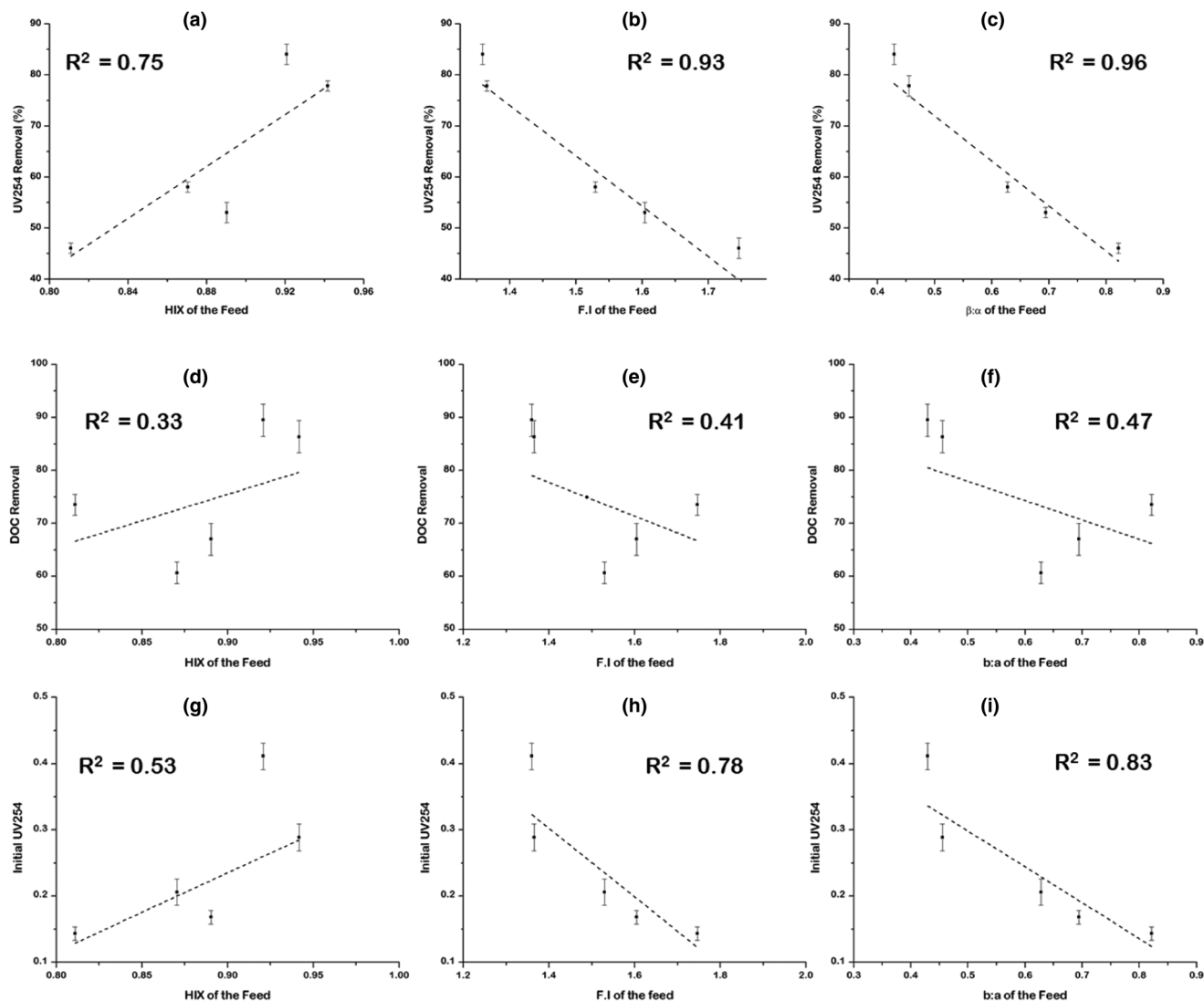
FIGURE 8 Correlation of spectroscopic indices with bulk parameter removal (a–c) UV_{254} removal, (d–f) DOC removal, and (g–i) initial UV_{254}. Experimental conditions: permeate sampling time: every hour; treatment time: 8 h; TMP: 3 bar; flux: 130 LMH. Pooled data from sites: H, Debose Dam; PL, Keubooms River; HL, Hezelmere River; MV, Vaal River; OL, Lepelle River

Influence of initial water quality parameters on *DOC* removal by ceramic membranes

Pearson correlation

Raw water quality parameters influences on the efficiency of *DOC* removal by the ceramic membranes was tested using Pearson correlation matrix (Table 3). Positive correlations existed between *DOC* removal and UV_{254} ($r = 0.79$) and *SUVA* ($r = 0.94$). Further, *DOC* removal had positive correlations with polarity-based fractions: *HPO* ($r = 0.65$), HPI ($r = 0.75$), and *TPI* ($r = 0.73$). Interestingly, spectroscopic indices such as *FI* and *β:α* had negative correlations with *DOC* removal ($r = -0.64$ and -0.69, respectively), whereas *HIX* had a positive

correlation with *DOC* removal by ceramic membranes ($r = 0.57$).

As demonstrated in Section 3.1, the quantity of *DOC* in the sample is not sufficient as a predictor for the rate of *DOC* removal; rather, other factors such as the chemistry of the organic matter in the feed water can have a bearing on the rate of *DOC* removal. As shown here, the rate of *DOC* removal correlated well with polarity-based fractions. Further, previous studies report terrestrially derived *NOM* ($FI \approx 1.7$) susceptibility to removal by ceramic membranes is less than that of microbial derived *NOM* ($FI \approx 1.4$) (Lidén et al., 2017). In this study, *FI* ranged from 1.3 to 1.7, suggesting a lower propensity to removal by ceramic membranes, conversely resulting in a negative correlation with the rate of *DOC* removal. A previous study reported similar findings that when the *FI*
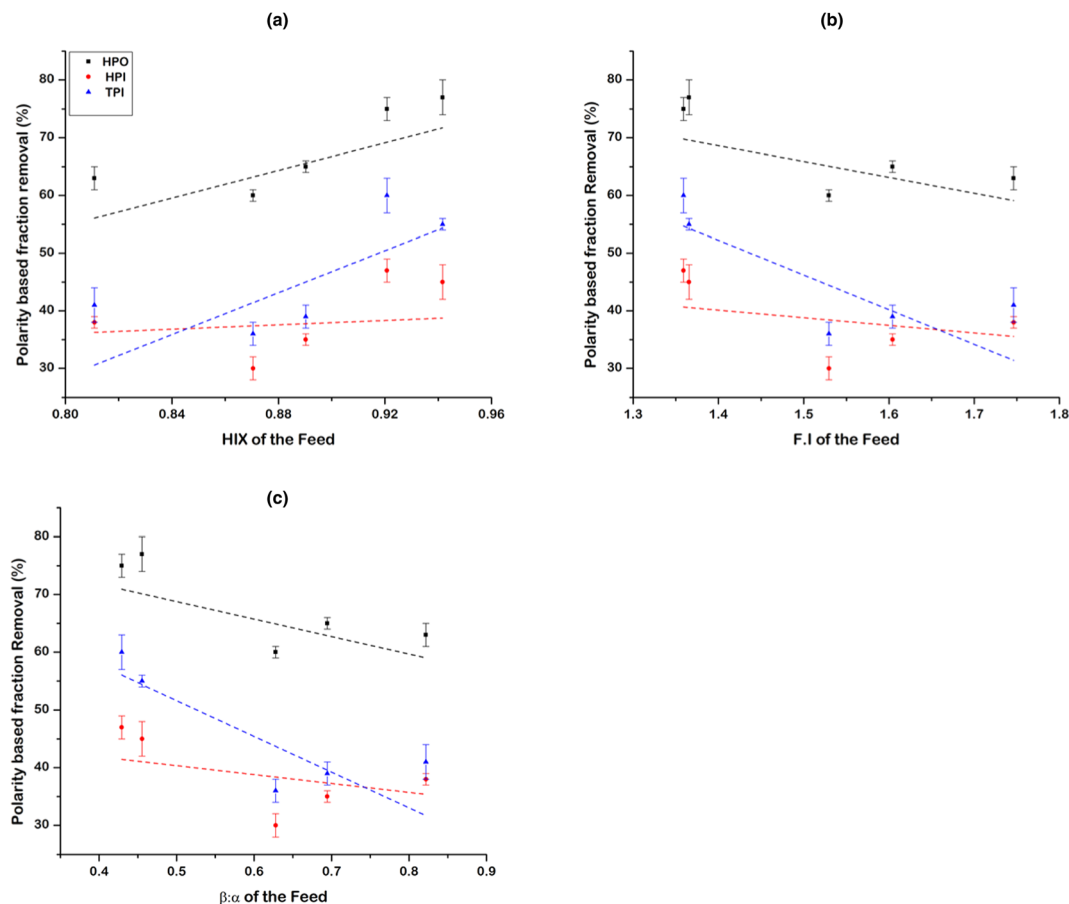
FIGURE 9 Correlations of spectroscopic indices with polarity based fraction removals: (a) *HIX* and polarity based fractions; (b) *FI* and polarity-based fractions and (c) *β:α* and polarity based fractions. Experimental conditions: permeate sampling time: every hour; treatment time: 8 hours; TMP: 3 bar; flux: 130 LMH. Pooled data from sites: H, Debose Dam; PL, Keubooms River; HL, Hezelmere River; MV, Vaal River; OL, Lepelle River

TABLE 3 Pearson correlations testing the influence of initial water parameters on DOC removal by ceramic membranes

	DOC removal	Initial DOC	Initial UV254	Initial BDOC	Initial SUVA	HIX of feed	FI of feed	β:α of feed	HPO of feed	HPI of feed	TPI of feed
DOC removal	-										
Initial DOC	0.403	-									
Initial UV254	0.788	0.849	-								
Initial BDOC	−0.086	0.382	0.062	-							
Initial SUVA	0.944	0.546	0.905	−0.148	-						
HIX of feed	0.574	0.684	0.734	0.584	0.655	-					
FI of feed	−0.643	−0.880	−0.885	−0.511	−0.726	−0.933	-				
β:α of feed	−0.688	−0.877	−0.914	−0.453	−0.771	−0.921	0.997	-			
HPO of feed	0.652	0.921	0.882	0.450	0.683	0.760	−0.938	−0.942	-		
HPI of feed	0.748	0.875	0.988	0.030	0.860	0.647	−0.848	−0.877	0.893	-	
TPI of feed	0.733	0.883	0.984	0.031	0.846	0.635	−0.842	−0.871	0.895	1.000	-

index of raw water was greater than 1.5, the *NOM* in that water was less susceptible to removal by ultrafiltration membranes (Lidén et al., 2017). Surface water containing

aged and condensed humic substances is characterized by low β:α; such water is amenable to removal by coagulation or membrane filtration (Lidén, 2017). The poor

correlations existed between the spectroscopic indices and *DOC* removal affirms the fact that the indices describe portions of the *DOC* (hence the heterogeneity) not necessarily representative of all the organic matter in the sample.

The understanding of fundamental fouling mechanisms involved during the filtration process of surface waters is pivotal in order to advance the use of ceramic membranes in water treatment. From Table 1, it can be noted that coastal plants had relatively high initial *DOC*, UV_{254}, and *SUVA* values compared with the inland plants. Further, in this work, we have established the influence of raw water quality parameters on *DOC* removal, and we have noted interesting correlations such as that of polarity-based fractions of the raw water having a bearing on the *DOC* removal. The next section delves on the role of such fractions on fouling mechanisms on ceramic membranes and how they can be used as predictors for the extent of fouling.

Loss of permeate flux and fouling mechanism of different waters on ceramic membranes

The effect of the physicochemical properties of water on fouling resistance is shown in Figure 10a. Plants MV and

PL had the similar rates of fouling in the first 75 min, followed by a steady state for the subsequent 30–40 min. However, the rate of *UV* transmission was different within the same time frames for both plants (Figure 10b). *UV* transmission decreased for MV although it remained constant for PL. This suggests the mechanism of fouling was different, probably depending on the character of NOM in each of the sites. Several theoretical models of flow reduction based on blocking mechanisms have been proposed (de Angelis et al., 2013; Lee et al., 2013; Mohammad et al., 2015; Teychene et al., 2016). These models describe four possible mechanisms, namely, cake filtration, complete blocking, intermediate blocking, and standard blocking. Usually, individual models cannot completely explain the variation of flux with time, but rather a combination of mechanisms is present.

The size of the solutes relative to the pores of the membrane determines the extent and progression of each mechanism. For molecules smaller than the mean pore size of the membrane, intermediate blocking is expected to dominate the fouling at the initial phase, and the subsequent stage is dominated by cake filtration fouling mechanism (de Angelis et al., 2013). The dominant fouling mechanisms for PL were intermediate fouling and cake filtration (R^2 of 0.85 and 0.83, respectively) (Table 4). Thus, the *UV* transmission was constant because after intermediate fouling the cake layer did not
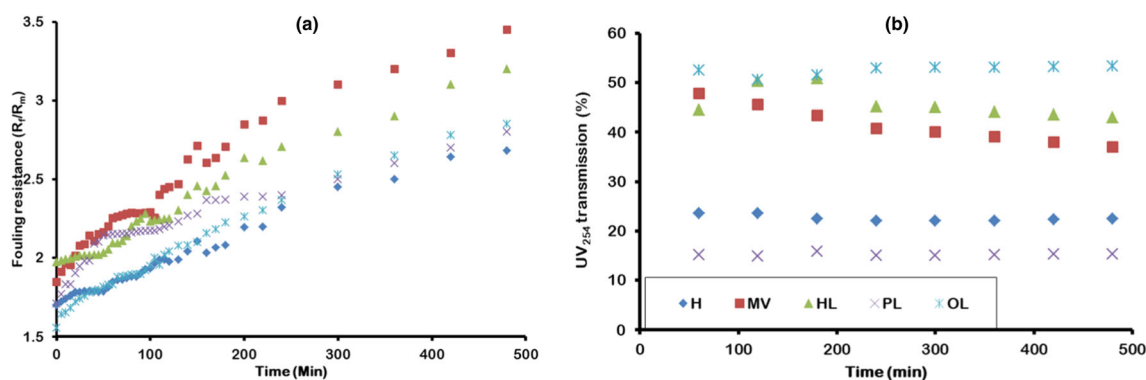

FIGURE 10 (a) Fouling resistance development during filtration of water from different sites and (b) UV–Vis transmission during filtration of waters from different sites. Experimental conditions: permeate sampling: every hour; treatment time: 8 h; TMP: 3 bar; flux: 130 LMH. Sites: H, Debose Dam; PL, Keubooms River; HL, Hezelmere River; MV, Vaal River; OL, Lepelle River

TABLE 4 Summary of the closeness of fit (R^2) of different fouling mechanism of water collected in different regions of South Africa

	Complete blocking	Standard blocking	Cake filtration	Intermediate blocking
H	0.24	0.23	0.78	0.68
MV	0.94	0.94	0.98	0.79
HL	0.96	0.89	0.80	0.65
PL	0.40	0.40	0.83	0.85
OL	0.42	0.41	0.97	0.90

TABLE 5 Pearson correlation of the influence of the initial water quality parameters on the extent of fouling

	DOC removal	Initial DOC	Initial UV	Initial BDOC	Initial SUVA	HIX of feed	FI of feed	b:a of feed	HPO of feed	HPI of feed	TPI of feed	Cake filtration	Complete blocking	Fouling resistance
DOC removal	-													
Initial DOC	0.403	-												
Initial UV	0.788	0.849	-											
Initial BDOC	−0.086	0.382	0.062	-										
Initial SUVA	0.944	0.546	0.905	−0.148	-									
HIX of feed	0.574	0.684	0.734	0.584	0.655	-								
FI of feed	−0.643	−0.880	−0.885	−0.511	−0.726	−0.933	-							
β:α of feed	−0.688	−0.877	−0.914	−0.453	−0.771	−0.921	0.997	-						
HPO of feed	0.652	0.921	0.882	0.450	0.683	0.760	−0.938	−0.942	-					
HPI of feed	0.748	0.875	0.988	0.030	0.860	0.647	−0.848	−0.877	0.893	-				
TPI of feed	0.733	0.883	0.984	0.031	0.846	0.635	−0.842	−0.871	0.895	1.000	-			
Cake filtration	−0.586	−0.194	−0.472	−0.283	−0.631	−0.823	0.605	0.608	−0.335	−0.334	−0.309	-		
Complete blocking	−0.877	−0.161	−0.494	0.076	−0.679	−0.255	0.367	0.408	−0.497	−0.495	−0.484	0.271	-	
Fouling resistance	−0.911	−0.030	−0.469	0.172	−0.744	−0.304	0.328	0.374	−0.368	−0.431	−0.413	0.469	0.954	-

allow any further significant amounts of *NOM* to pass though the membrane. For MV, all fouling mechanisms had almost equal contribution on fouling (for complete blocking, standard blocking, cake filtration, and intermediate blocking, with $R^2 = 0.94$, 0.94, 0.98, and 0.79, respectively). However, the *UV* transmission of MV was higher than that of PL, implying fouling was severe with PL than MV.

Plants H, HL, and OL showed similar fouling rates in the first 3 h (Figure 10a). However, the rates of *UV* transmission at that time frame were different. Complete blocking and standard fouling were the dominant fouling mechanisms for HL ($R^2 = 0.96$ and 0.89, respectively) (Table 4). As the buildup of fouling progressed, the *UV* transmission in the first 3 h increased, suggesting *NOM* particles smaller than the pores of the membranes were passing through, and HL probably had *NOM* molecules small enough to pass through the pores compared with *NOM* from other sites. Further verification of the molecular size distribution of *NOM* found in these sites should be investigated.

Whereas for OL and H there was a constant *UV* transmission within the first 3 h and there was an initial increase in UV transmission for HL, implying cake filtration was the least fouling mechanism within that time frame (Figure 10b). However, UV transmission for OL was higher than for all the other sites, implying OL least fouled the ceramic membranes compared to the other sites. Complete blocking ($R^2 = 0.24$ and 0.42 for H and OL, respectively) and standard blocking ($R^2 = 0.23$ and 0.41 for H and OL, respectively) were the least fouling mechanisms for H and OL. Intermediate blocking ($R^2 = 0.68$ and 0.90 for H and OL, respectively) and cake filtration ($R^2 = 0.78$ and 0.97 for H and OL, respectively) were the dominant fouling mechanisms. This implies for H and OL an initial phase dominated by intermediate blocking was followed by a transition to cake filtration at a subsequent stage in the filtration process.

Influence of initial water quality parameters on the extent of fouling

Pearson correlation analysis

Raw water quality parameters influences on the main fouling mechanisms (cake filtration and complete blocking) and fouling resistance was tested using Pearson correlation matrix (Table 5). There was a negative correlation between the models of fouling and the rate of *DOC* removal ($r = -0.59$ for cake filtration and -0.89 for complete blocking), suggesting, as the *DOC* was being removed, it did not necessarily imply the organic matter

was settling on the ceramic membrane surface and influencing the formation of a cake layer or complete blocking; specifically, rather all fouling mechanisms were at play. Very weak negative correlations were observed between the initial *DOC* and fouling models ($r = -0.19$ and -0.16 for cake filtration and complete blocking, respectively); further, a weakly negative correlation was observed between initial *DOC* and fouling resistance ($r = -0.03$). These findings suggest fouling is not purely depended on the quantity of *DOC*, but other factors such as hydrodynamic parameters such as transmembrane pressure; flow rate; solution physicochemical properties such as pH, ionic strength and temperature; and membrane properties such as hydrophilicity and pore size (Tylkowski & Tsibranska, 2015).

Positive correlations were observed between the fouling models and spectroscopic indices such as *FI* ($r = 0.61$ and 0.37 for cake filtration and complete blocking, respectively) and $\beta{:}\alpha$ ($r = 0.61$ and 0.41 for cake filtration and complete blocking, respectively). Again, positive correlations were observed between fouling resistance and spectroscopic indices such as *FI* ($r = 0.33$) and $\beta{:}\alpha$ ($r = 0.37$). Interestingly, negative correlations existed between cake filtration fouling indices and polarity based fractions ($r = -0.34$, -0.33, and -0.31 for *HPO*, *HPI*, and *TPI*, respectively) and similarly between complete blocking and polarity based fractions ($r = -0.5$, -0.5, and -0.49 for *HPO*, *HPI*, and *TPI*, respectively). This implies polarity on its own was not a strong factor in influencing fouling. These results reiterate the multifaceted nature of fouling by organic matter found in surface waters.

CONCLUSION

The rate of removal of bulk NOM (measured as UV_{254} and *DOC* removal), the *BDOC* fraction, polarity fractions, and *FDOM* fractions was investigated, and the key findings were as follows:

1. Ceramic membranes were more effective in removing bulk *NOM* for coastal plants than inland plants mainly because coastal had relatively high *DOC* values compared with inland plants.
2. The removal of *FDOM* did not depend on the location of the WTP.
3. The removal of *BDOC* was high for coastal plants and correlated well with *DOC* removal. Thus, *DOC* removal can be an indicator to predict BDOC removal.
4. The *HPO* fraction was the most amenable to removal by ceramic membranes regardless of the site of the WTP. *UV* transmission for *OL* was higher than all the

other sites, implying OL waters least fouled the ceramic membranes compared with the other sites.

This investigation revealed the dynamics of *NOM* fraction removal by ceramic membranes, specific to South African waters, and the results serve as an initial appraisal for the application of ceramic membranes in removing *NOM* fractions in South Africa.

AUTHOR CONTRIBUTIONS
Welldone Moyo: Conceptualization; data curation; formal analysis; investigation; methodology. **Machawe M. Motsa:** Conceptualization; data curation; formal analysis; methodology. **Nhamo Chaukura:** Conceptualization; data curation; formal analysis. **Titus A.M Msagati:** Funding acquisition; investigation; methodology. **Bhekie B. Mamba:** Funding acquisition; methodology; project administration; supervision; visualization. **Sebastiaan G.J Heijman:** Conceptualization; formal analysis; investigation; methodology; supervision. **Thabo T.I Nkambule:** Funding acquisition; investigation; methodology; project administration; supervision.

DATA AVAILABILITY STATEMENT
Data available on request from the authors.

ORCID
Welldone Moyo https://orcid.org/0000-0003-0341-2919

REFERENCES
Baghoth, S. A., Sharma, S. K., & Amy, G. L. (2010). Tracking natural organic matter (NOM) in a drinking water treatment plant using fluorescence excitation e emission matrices and PARAFAC. *Water Research*, *45*(2), 797–809. https://doi.org/10.1016/j.watres.2010.09.005

Bieroza, M., Baker, A., & Bridgeman, J. (2011). Exploratory analysis of excitation–emission matrix fluorescence spectra with self-organizing maps—A tutorial. *Education for Chemical Engineers*, *7*(1), 22–31. https://doi.org/10.1016/j.ece.2011.10.002

Cawley, K. M., Ding, Y., Fourqurean, J. W., & Jaffé, R. (2012). Characterising the sources and fate of dissolved organic matter in Shark Bay, Australia: A preliminary study using optical properties and stable carbon isotopes. *Marine and Freshwater Research*, *63*, 1098–1107. https://doi.org/10.1071/MF12028

Chae, S. R., Noeiaghaei, T., Jang, H. C., Sahebi, S., Jassby, D., Shon, H. K., Park, P. K., Kim, J. O., & Park, J. S. (2015). Effects of natural organic matter on separation of the hydroxylated fullerene nanoparticles by cross-flow ultrafiltration membranes from water. *Separation and Purification Technology*, *140*, 61–68. https://doi.org/10.1016/j.seppur.2014.11.011

Chaukura, N., Ndlangamandla, N. G., Moyo, W., Msagati, T. A. M., Mamba, B. B., & Nkambule, T. T. I. (2018). Natural organic matter in aquatic systems – A South African perspective. *Water SA*, *44*(4), 624–635. https://doi.org/10.4314/wsa.v44i4.11

Chen, C., Leavey, S., Krasner, S. W., & Suffet, I. H. (2014). Applying polarity rapid assessment method and ultrafiltration to characterize NDMA precursors in wastewater effluents. *Water Research*, *57*, 115–126. https://doi.org/10.1016/j.watres.2014.02.052

Chen, Z., Li, M., Wen, Q., & Ren, N. (2017). Evolution of molecular weight and fluorescence of effluent organic matter (EfOM) during oxidation processes revealed by advanced spectrographic and chromatographic tools. *Water Research*, *124*, 566–575. https://doi.org/10.1016/j.watres.2017.08.006

de Angelis, L., Marta, M., & de Cortalezzi, F. (2013). Ceramic membrane filtration of organic compounds: Effect of concentration, pH, and mixtures interactions on fouling. *Separation and Purification Technology*, *118*, 762–775. https://doi.org/10.1016/j.seppur.2013.08.016

Escobar, I. C., & Randall, A. A. (2001). Assimilable organic carbon (aoc) and biodegradable dissolved organic carbon (bdoc): Complementary measurements. *Water Research*, *35*(18), 4444–4454. https://doi.org/10.1016/S0043-1354(01)00173-7

Fang, L. F., Kato, N., Yang, H. Y., Cheng, L., Hasegawa, S., Jeon, S., & Matsuyama, H. (2018). Evaluating the antifouling properties of poly(ether sulfone)/sulfonated poly(ether sulfone) blend membranes in a full-size membrane module. *Industrial and Engineering Chemistry Research*, *57*(12), 4430–4441. https://doi.org/10.1021/acs.iecr.8b00114

He, X. S., Xi, B. D., Li, X., Pan, H. W., An, D., Bai, S. G., Li, D., & Cui, D. Y. (2013). Fluorescence excitation-emission matrix spectra coupled with parallel factor and regional integration analysis to characterize organic matter humification. *Chemosphere*, *93*(9), 2208–2215. https://doi.org/10.1016/j.chemosphere.2013.04.039

Henderson, R. K., Baker, A., Murphy, K. R., Hambly, A., Stuetz, R. M., & Khan, S. J. (2009). Fluorescence as a potential monitoring tool for recycled water systems: A review. *Water Research*, *43*(4), 863–881. https://doi.org/10.1016/j.watres.2008.11.027

Hofs, B., Ogier, J., Vries, D., Beerendonk, E. F., & Cornelissen, E. R. (2011). Comparison of ceramic and polymeric membrane permeability and fouling using surface water. *Separation and Purification Technology*, *79*(3), 365–374. https://doi.org/10.1016/j.seppur.2011.03.025

Hua, G., Reckhow, D. A., & Abusallout, I. (2015). Correlation between SUVA and DBP formation during chlorination and chloramination of NOM fractions from different sources. *Chemosphere*, *130*, 82–89. https://doi.org/10.1016/j.chemosphere.2015.03.039

Kastl, G., Sathasivan, A., & Fisher, I. (2016). A selection framework for NOM removal process for drinking water treatment. *Desalination and Water Treatment*, *3994*, 1–11. https://doi.org/10.1080/19443994.2015.1044476

Knowles, A. D. (2011). Optimizing the removal of natural organic matter in drinking water while avoiding unintended

consequences following coagulation. PhD Thesis, Dalhousie University.

Korak, J. A., Dotson, A. D., Summers, R. S., & Rosario-ortiz, F. L. (2013). Critical analysis of commonly used fluorescence metrics to characterize dissolved organic matter. *Water Research*, *49*, 327–338. https://doi.org/10.1016/j.watres.2013.11.025

Krzeminski, P., Vogelsang, C., Meyn, T., Köhler, S. J., Poutanen, H., de Wit, H. A., & Uhl, W. (2019). Natural organic matter fractions and their removal in full-scale drinking water treatment under cold climate conditions in Nordic capitals. *Journal of Environmental Management*, *241*, 427–438. https://doi.org/10.1016/j.jenvman.2019.02.024

Lavonen, E. (2015). Tracking changes in dissolved natural organic matter composition. Doctoral Thesis, Swedish University of Agricultural Sciences.

Lee, S. J., Dilaver, M., Park, P. K., & Kim, J. H. (2013). Comparative analysis of fouling characteristics of ceramic and polymeric microfiltration membranes using filtration models. *Journal of Membrane Science*, *432*, 97–105. https://doi.org/10.1016/j.memsci.2013.01.013

Li, W. T., Cao, M. J., Young, T., Ruffino, B., Dodd, M., Li, A. M., & Korshin, G. (2017). Application of UV absorbance and fluorescence indicators to assess the formation of biodegradable dissolved organic carbon and bromate during ozonation. *Water Research*, *111*, 154–162. https://doi.org/10.1016/j.watres.2017.01.009

Li, P., & Hur, J. (2017). Utilization of UV-vis spectroscopy and related data analyses for dissolved organic matter (DOM) studies: A review. *Critical Reviews in Environmental Science and Technology*, *47*(3), 131–154. https://doi.org/10.1080/10643389.2017.1309186

Liao, X., Bei, E., Li, S., Ouyang, Y., Wang, J., Chen, C., Zhang, X., Krasner, S. W., & Suffet, I. H. M. (2015). Applying the polarity rapid assessment method to characterize nitrosamine precursors and to understand their removal by drinking water treatment processes. *Water Research*, *87*, 292–298. https://doi.org/10.1016/j.watres.2015.09.040

Lidén, A., Keucken, A., & Persson, K. M. (2017). Journal of water process engineering uses of fluorescence excitation-emissions indices in predicting water treatment efficiency. *Journal of Water Process Engineering*, *16*, 249–257. https://doi.org/10.1016/j.jwpe.2017.02.003

Lobanga, K. P., Haarhoff, J., & van Staden, S. J. (2013). Treatability of South African surface waters by enhanced coagulation. *Water SA*, *39*(3), 379–384. https://doi.org/10.4314/wsa.v39i3.6

Lyon, B. A., Cory, R. M., & Weinberg, H. S. (2014). Changes in dissolved organic matter fluorescence and disinfection byproduct formation from UV and subsequent chlorination/chloramination. *Journal of Hazardous Materials*, *264*, 411–419. https://doi.org/10.1016/j.jhazmat.2013.10.065

Marais, S. S., Ncube, E. J., Msagati, T. A., Mamba, B. B., & Nkambule, T. T. (2017). Investigation of natural organic matter (NOM) character and its removal in a chlorinated and chloraminated system at Rand water, South Africa. *Water Supply*, *17*, 1287–1297. https://doi.org/10.2166/ws.2017.028

Metsämuuronen, S., Sillanpää, M., Bhatnagar, A., & Mänttäri, M. (2014). Natural organic matter removal from drinking water by membrane technology. *Separation and Purification Technology*, *43*, 1–61. https://doi.org/10.1080/15422119.2012.712080

Mohammad, A. W., Teow, Y. H., Ang, W. L., Chung, Y. T., Oatley-Radcliffe, D. L., & Hilal, N. (2015). Nanofiltration membranes review: Recent advances and future prospects. *Desalination*, *356*, 226–254. https://doi.org/10.1016/j.desal.2014.10.043

Moyo, W., Chaukura, N., Motsa, M. M., Msagati, T. A. M., Mamba, B. B., & Heijman, S. G. J. (2020). Investigating the fate of natural organic matter at a drinking water treatment plant in South Africa using optical spectroscopy and chemometric analysis. *Water SA*, *46*(1), 131–140.

Moyo, W., Chaukura, N., Msagati, T. A. M., & Mamba, B. B. (2019). The properties and removal efficacies of natural organic matter fractions by South African drinking water treatment plants. *Journal of Environmental Chemical Engineering*, *7*(3), 103101. https://doi.org/10.1016/j.jece.2019.103101

Murphy, K. R., Hambly, A., Singh, S., Henderson, R. K., Baker, A., Stuetz, R., & Khan, S. J. (2011). Organic matter fluorescence in municipal water recycling schemes: Toward a unified PARAFAC model. *45*(7), 2909–2916. https://doi.org/10.1021/es103015e

Murphy, K. R., Stedmon, C. A., Wenig, P., & Bro, R. (2014). OpenFluor – An online spectral library of auto-fluorescence by organic compounds in the environment. *Analytical Methods*, *6*(3), 658–661. https://doi.org/10.1039/c3ay41935e

Ndiweni, S. N., Chys, M., Chaukura, N., Van Hulle, S. W., & Nkambule, T. T. (2019). Assessing the impact of environmental activities on natural organic matter in South Africa and Belgium. *Environmental Technology*, *40*, 1756–1768. https://doi.org/10.1080/09593330.2019.1575920

Nescerecka, A., Juhna, T., & Hammes, F. (2018). Identifying the underlying causes of biological instability in a full-scale drinking water supply system. *Water Research*, *135*, 11–21. https://doi.org/10.1016/j.watres.2018.02.006

Nkambule, T. I., Krause, R. W. M., Haarhoff, J., & Mamba, B. B. (2012). Natural organic matter (NOM) in South African waters: Characterization of NOM, treatability and method development for effective nom removal from water. Ph.D Thesis, University of Johannesburg.

Osburn, C. L., Boyd, T. J., Montgomery, M. T., Bianchi, T. S., Coffin, R., & Paerl, H. W. (2016). Optical proxies for terrestrial dissolved organic matter in estuaries and coastal waters. *Frontiers in Marine Science*, *2*, 127. https://doi.org/10.3389/fmars.2015.00127

Osburn, C. L., Handsel, L. T., Mikan, M. P., Paerl, H. W., & Montgomery, M. T. (2012). Fluorescence tracking of dissolved and particulate organic matter quality in a river-dominated estuary. *Environmental Science & Technology*, *46*(16), 8628–8636. https://doi.org/10.1021/es3007723

Park, J. W., Kim, H.-C., Meyer, A. S., Kim, S., & Maeng, S. K. (2016). Influences of NOM composition and bacteriological characteristics on biological stability in a full-scale drinking water treatment plant. *Chemosphere*, *160*, 189–198. https://doi.org/10.1016/j.chemosphere.2016.06.079

Pendergast, M. M., & Hoek, E. M. V. (2011). A review of water treatment membrane nanotechnologies. *Energy & Environmental Science*, *4*(6), 1946. https://doi.org/10.1039/c0ee00541j

Sanchez, N. P., Skeriotis, A. T., & Miller, C. M. (2013). Assessment of dissolved organic matter fluorescence PARAFAC components before and after coagulation e filtration in a full scale

water treatment plant. *Water Research*, *47*(4), 1679–1690. https://doi.org/10.1016/j.watres.2012.12.032

Shang, R. (2014). Ceramic ultra- and nanofiltration for municipal wastewater reuse.

Shang, R., Goulas, A., Tang, C. Y., de Frias Serra, X., Rietveld, L. C., & Heijman, S. G. J. (2017). Atmospheric pressure atomic layer deposition for tight ceramic nanofiltration membranes: Synthesis and application in water purification. *Journal of Membrane Science*, *528*, 163–170. https://doi.org/10.1016/j.memsci.2017.01.023

Terry, L. G., & Summers, R. S. (2018). Biodegradable organic matter and rapid-rate bio filter performance: A review. *Water Research*, *128*, 234–245. https://doi.org/10.1016/j.watres.2017.09.048

Teychene, B., Collet, G., & Gallard, H. (2016). Modeling of combined particles and natural organic matter fouling of ultrafiltration membrane. *Journal of Membrane Science*, *505*, 185–193. https://doi.org/10.1016/j.memsci.2016.01.039

Tijani, J. O., Fatoba, O. O., Madzivire, G., & Petrik, L. F. (2014). A review of combined advanced oxidation technologies for the removal of organic pollutants from water. *Water, Air, and Soil Pollution*, *225*(9), 1–30. https://doi.org/10.1007/s11270-014-2102-y

Trubetskaya, O. E., Richard, C., & Trubetskoj, O. A. (2016). High amounts of free aromatic amino acids in the protein-like fluorescence of water-dissolved organic matter. *Environmental Chemistry Letters*, *14*, 495–500. https://doi.org/10.1007/s10311-016-0556-4

Tshindane, P., Mamba, P. P., Moss, L., Swana, U. U., Moyo, W., Motsa, M. M., Chaukura, N., Mamba, B. B., & Nkambule, T. T. I. (2019). The occurrence of natural organic matter in South African water treatment plants. *Journal of Water Process Engineering*, *31*, 100809. https://doi.org/10.1016/j.jwpe.2019.100809

Tylkowski, B., & Tsibranska, I. (2015). Overview of main techniques used for membrane characterization. *Journal of Chemical Technology and Metallurgy*, *50*(1), 3–12.

Virtanen, T., Parkkila, P., Koivuniemi, A., Lahti, J., Viitala, T., Kallioinen, M., Mänttäri, M., & Bunker, A. (2018). Characterization of membrane–foulant interactions with novel combination of Raman spectroscopy, surface plasmon resonance and molecular dynamics simulation. *Separation and Purification Technology*, *205*, 263–272. https://doi.org/10.1016/j.seppur.2018.05.050

Vital, M., Stucki, D., Egli, T., & Hammes, F. (2010). Evaluating the growth potential of pathogenic bacteria in water. *Applied and Environmental Microbiology*, *76*(19), 6477–6484. https://doi.org/10.1128/AEM.00794-10

Wang, L., & Benjamin, M. M. (2016). A multi-spectral approach to differentiate the effects of adsorbent pretreatments on the characteristics of NOM and membrane fouling. *Water Research*, *98*, 56–63. https://doi.org/10.1016/j.watres.2016.03.066

Wünsch, U. J., Murphy, K. R., & Stedmon, C. A. (2017). The one-sample PARAFAC approach reveals molecular size distributions of fluorescent components in dissolved organic matter. *Environmental Science & Technology*, *51*(20), 11900–11908. https://doi.org/10.1021/acs.est.7b03260

Yamashita, Y., Kloeppel, B. D., Knoepp, J., Zausen, G. L., & Jaffe, R. (2011). Effects of watershed history on dissolved organic matter characteristics in headwater streams. *Ecosystems*, *14*, 1110–1122. https://doi.org/10.1007/s10021-011-9469-z

Zhang, Y., Zhao, X., Zhang, X., & Peng, S. (2015). A review of different drinking water treatments for natural organic matter removal. *Water Science & Technology: Water Supply*, *15*(3), 442–455. https://doi.org/10.2166/ws.2015.011

Zularisam, A. W., Ismail, A. F., Salim, M. R., Sakinah, M., & Ozaki, H. (2007). The effects of natural organic matter (NOM) fractions on fouling characteristics and flux recovery of ultrafiltration membranes. *Desalination*, *212*(1–3), 191–208. https://doi.org/10.1016/j.desal.2006.10.010